

# All optical thrombotic stroke model for near-surface blood vessels in rat: Focal illumination of exogenous photosensitizers combined with real-time two-photon imaging

Chris B. Schaffer<sup>1,a</sup>, Philbert S. Tsai<sup>a</sup>, Nozomi Nishimura<sup>a</sup>, Lee F. Schroeder<sup>b</sup>, Beth Friedman<sup>b</sup>,  
Patrick D. Lyden<sup>b,c</sup>, Ford F. Ebner<sup>d</sup>, and David Kleinfeld<sup>a,c</sup>

<sup>a</sup>Department of Physics, University of California, San Diego

<sup>b</sup>Department of Neurosciences, School of Medicine, University of California, San Diego

<sup>c</sup>Graduate Program in Neurosciences, University of California, San Diego

<sup>d</sup>Department of Psychology, Vanderbilt University

## ABSTRACT

Photothrombotic microstrokes are produced in rat cortex by 532-nm single-photon optical excitation of an intravenously injected photosensitizer, rose bengal. The dynamics of blood flow and clot formation in the cortical vasculature are observed using two-photon laser scanning microscopy of an intravenously injected fluorescent dye. Flowing and clotted vessels are clearly distinguishable in both large and small vessels, down to individual capillaries, using this technique. We find that by tightly focusing the laser light used to excite the photosensitizer, clots can be formed in individual blood vessels without affecting neighboring vessels tens of micrometers away. We observe many changes in blood flow as a result of localized clot formation, including upstream vascular dilation, clot clearing, i.e. recanalization, and complete reversal of blood flow direction downstream.

Keywords: two-photon laser scanning microscopy, photosensitizer, cortical microvasculature, cerebral ischemia, photothrombosis, stroke

## 1. INTRODUCTION

Options for the treatment of stroke remain few and of limited efficacy despite years of basic and clinical research. Future progress depends critically on animal models that allow ischemic stroke to be studied at various stages, from initial changes in blood flow, to the physiological reaction to ischemia, to neuronal death, to behavioral impairment and recovery. Most stroke models developed to date focus on events that occur from hours to days after ischemic injury. Here we report on a model for thrombotic stroke in near-surface vessels that allows direct observation of events occurring in the vasculature on the timescale of minutes to hours.

### *Past models of stroke:*

Stroke models rely on a number of methods to reduce blood flow to the brain, but few are well suited to the study of blood flow and vessel dynamics soon after blood flow is reduced. Many models rely on the ligation of large arteries (1) or microsurgical occlusion of smaller arteries, such as the middle cerebral artery (2-6). Internal blockage of the middle cerebral artery by insertion of a string through the carotid artery has also been demonstrated (7,8). These mechanical occlusion techniques, while producing ischemia-induced lesions, offer limited insight into the blood flow dynamics that occur during a thrombotic stroke (9,10). Injection of pre-formed clots (11-13) or micrometer-sized beads (14-16) into the bloodstream leads to clots downstream from the injection site. The inability to predict where the clot will lodge, however, makes it very difficult to monitor blood flow in the appropriate area.

Optical excitation of exogenous photosensitizer molecules has also been shown to be effective in producing clots and ischemia-induced lesions (17-19). In this model, an intravenously injected photosensitizer, such as the fluorescein derivative rose bengal, is optically excited. Photosensitizers have a high probability of undergoing intersystem crossing

---

<sup>1</sup> cschaffer@ucsd.edu; Tel: 858 534 3562

from the excited singlet to the triplet state (20). Subsequent interaction with molecular oxygen, a molecule with a triplet ground state, leads to the formation of singlet oxygen and the recycling of the photosensitizer (20). Singlet oxygen is known to damage fatty acids and proteins in cell membranes (21). This results in injury to the endothelial wall of the vessel and leads to platelet aggregation and clot formation (17,22). This model for stroke has primarily been applied using widefield illumination of relatively large areas of the cortex (23).

*Past techniques for observing changes in blood flow:*

Changes in blood perfusion following vessel occlusion by either photochemically-induced or injected clots is typically determined by injecting a contrast agent, such as carbon black, into the blood stream and then performing routine histology on the excised brain (10,17,24). Clotted blood vessels are not filled with by the carbon black, allowing their identification. By sacrificing animals at different time points after the same procedure, a time course of the extent of the blockage and (possible) recovery of flow can be determined. Typically, effects are characterized on timescales of hours to days with these methods (23).

Recently, laser Doppler flowmetry (25), magnetic resonance imaging (26,27), fluorescent video microscopy (5,6,28), and confocal laser scanning fluorescence microscopy (29,30) have been used to characterize changes in blood flow after ischemic injury in real-time. With the exception of the light microscopy, these techniques are limited to determining average flow over sub-millimeter-sized areas, at best. While such an average may be relevant for determining the degree of ischemia, they provide no input on changes in flow and morphology in individual vessels. Fluorescent video microscopy allows individual vessels to be studied, but is limited to the observation of surface vessels only, while confocal microscopy allows vessels up to 100  $\mu\text{m}$  beneath the surface to be visualized. These observation techniques have allowed quantitative characterization of changes in blood flow velocity and blood vessel dilation as a result of large-scale ischemia produced by surgical occlusion of arteries and arterioles (4-6,29,30). These studies did not, however, address local changes in blood flow and vessels near an isolated occlusion. Recently, fluorescent video microscopy was used to study vessel response to photochemically-induced clots in individual arterioles, but the results were limited to surface vessels and have poor spatial resolution (28).

*Present work:*

In this report, we describe the use of tightly-focused laser illumination to optically excite a photosensitizer molecule, allowing precise localization of clot formation at the level of individual arterioles, venules, and capillary beds. Because we precisely localize the clot, we can study changes in blood vessels and blood flow both upstream and downstream from the clotted region and in neighboring vessels. We used two-photon laser scanning fluorescence microscopy to observe, in real-time, these changes in blood flow after clot formation (31). Two-photon microscopy has recently been used to characterize natural variability and stimulus-induced changes in blood flow in individual capillaries in rat neocortex at depth (32). This ability for localized, quantitative characterization of blood flow could become a powerful tool in the study of stroke. Two-photon microscopy also offers intrinsic optical sectioning, up to 500- $\mu\text{m}$  penetration depth (providing access to layers 1 – 4 of the cortex in rat), low photodamage, and the ability to maintain image resolution while imaging into scattering tissue, all providing greater flexibility in the study of changes in blood flow after localized clot formation (31-34).

## **2. EXPERIMENTAL PROCEDURES**

Six Sprague-Dawley rats, approximately 200 g in weight, were used in these pilot studies. The animal protocols follow those described previously (32) and were approved by the local Institutional Animal Care Committee. Briefly, the animals were anesthetized with urethane (1.5 g/kg animal weight, inter-peritoneal, supplemented as needed), and received atropine (0.05 mg/kg animal weight, sub-cutaneously every hour) and 5% (wt/vol) glucose in isotonic saline (10 ml/kg animal weight, sub-cutaneously every hour) throughout the experiment. A craniotomy was performed above parietal cortex and the dura was removed. A metal frame was fixed to the skull and held a coverslip over the exposed cortex. The region between the coverslip and cortical surface was filled with 1% (wt/vol) agarose in artificial cerebrospinal fluid (35). A coarse map of the vasculature was obtained by imaging the cortex surface onto a CCD camera with widefield green (centered at 530 nm) illumination (36). To fluorescently label the blood plasma, 0.5 ml of 5% (wt/vol) fluorescein isothiocyanate-labeled dextran (2 MDa) in isotonic saline was injected into either the tail vein or the saphenous vein in the leg.

The animal was placed in the setup shown in Fig. 1. Femtosecond pulses at 800-nm wavelength from a commercial laser oscillator (Mira, from Coherent, Inc., pumped by a 10-W diode-pumped solid state Nd:Vanadate laser, also from Coherent, Inc.) are directed to a home-built two-photon microscope (37). The femtosecond laser light is focused into the sample using a water immersion microscope objective (20 $\times$  magnification, 0.5 numerical aperture, Olympus). Fluorescence is collected by the same microscope objective and directed to a photomultiplier tube by a long-pass dichroic mirror. A short-pass filter prevents residual light from the femtosecond laser from reaching the detector. To build an image, the photomultiplier signal is recorded as a function time while the two galvanometric mirrors raster scan the focus of the femtosecond beam (giving  $x,y$  coordinates). The position of the microscope objective relative to the sample is also recorded (providing a  $z$  coordinate). In most of the data presented here, a succession of two-dimensional images of a vessel was recorded at a single  $z$ -position. Images were taken at a rate of a few frames per second. Where noted, two-dimensional projections of three-dimensional data are constructed by taking the maximal value of each pixel along the direction perpendicular to the plane of the image.

Under the two-photon microscope, candidate vessels for photochemical blockage were identified and their position noted. The animal was then given a second intravenous injection consisting of 0.8 ml 2% (wt/vol) fluorescein isothiocyanate-labeled dextran (2 MDa) and 3% (wt/vol) rose bengal in isotonic saline. To induce clot formation, the femtosecond laser beam is blocked and a 532-nm continuous wave laser beam from an intracavity frequency doubled Nd:YAG laser is introduced into the beam path using a flip-in mirror. The dichroic mirror is removed from the path, as it is reflective at 532 nm. The 532-nm beam is aligned so it focuses in the center of the field and at the same  $z$ -position that is imaged using two-photon microscopy. The average power of the 532-nm laser, measured after the microscope objective, was set to 10 mW, except where noted.

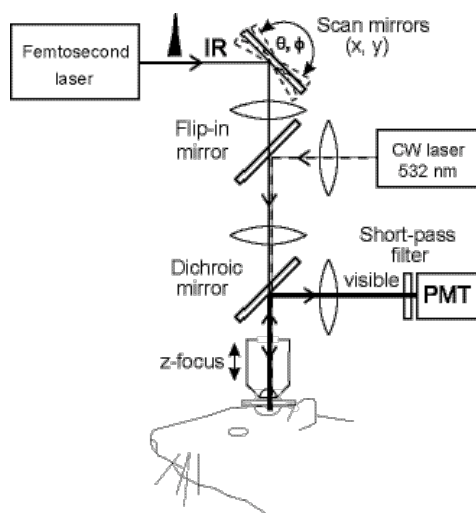


**Fig. 1.** Setup for production and observation of laser-induced thrombosis. Femtosecond laser pulses (800-nm wavelength) are directed via galvanometric scan mirrors through a water-immersion microscope objective (20 $\times$ , 0.5 NA, Olympus) into rat cortex. Two-photon excited fluorescence is collected on a photomultiplier tube while the position of the femtosecond laser focus is raster scanned inside the sample, forming an image. A short-pass filter prevents backscattered femtosecond pulses from reaching the detector. To optically excite rose bengal and produce thrombosis the femtosecond laser beam is blocked, the dichroic removed, and a continuous wave 532-nm laser beam is directed into the microscope objective using a flip-in mirror.

Laser exposure was conducted in 1-min. epochs, with observation by two-photon microscopy following each epoch. We generally found that 1 min. of irradiation consistently produced complete occlusion of vessels up to about 50  $\mu\text{m}$  in diameter, provided that the irradiation was performed soon after a rose bengal injection. The rose bengal concentration in the blood decreases with time and, after 1.5 to 2 hours, additional rose bengal must be injected in order to reliably produce a clot. Clotted vessels were re-imaged periodically at time points up to two hours after clot formation. As many as 10 different, isolated clots were produced and studied in each animal.

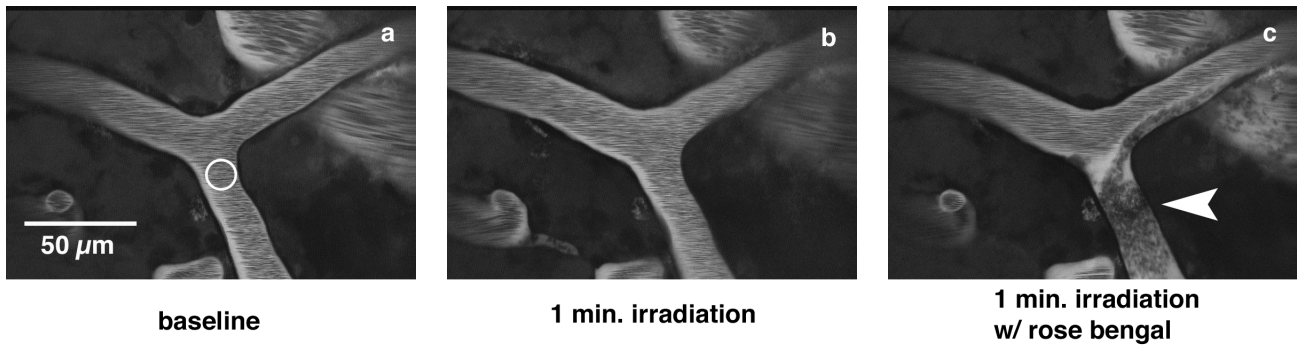
After the experiment two of the animals were perfused transcardially with 100 ml of isotonic saline solution, followed by 50 ml of 50- $\mu\text{M}$  5-hexadecanoylaminofluorescein, a fluorescent lipid analog, in isotonic saline with 0.5% ethanol, then 100 ml of 4% (wt/vol) paraformaldehyde in isotonic saline. The brains were removed and the cortex extracted. Fiducial marks were made with a straight pin to identify the location of the cortical window. The cortex was immobilized in 2% (wt/vol) agarose in isotonic saline and imaged on the two-photon microscope using a 100 $\times$  magnification, 1.0 numerical aperture water immersion objective (Olympus). The lipophilic fluorescein brightly labeled the inner wall of the blood vessels, allowing post-mortem visualization of the cortical vasculature. Clotted vessels show diffuse labeling in the vessel lumen and are readily distinguishable from normal vessels which show no labeling in the lumen.

### 3. RESULTS AND DISCUSSION

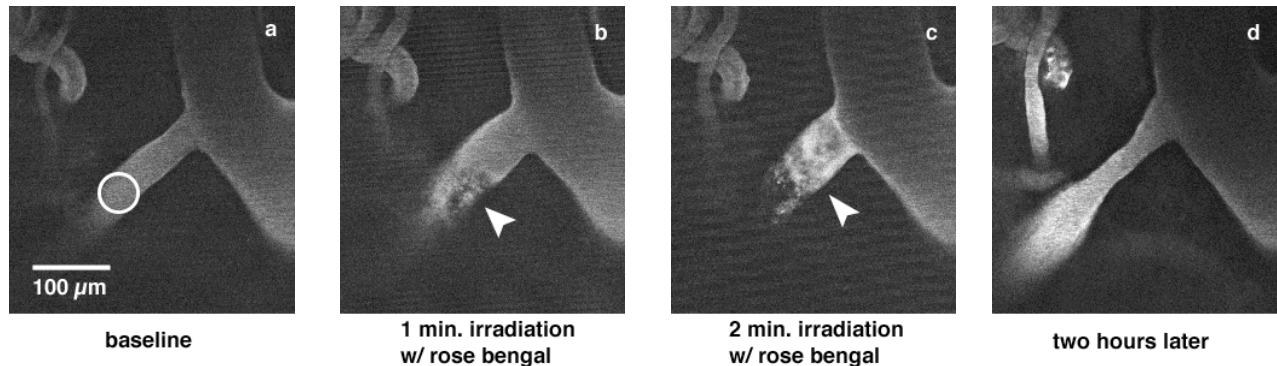
Two-photon laser scanning fluorescent microscopy was used to image the flow of red blood cells in cortical blood vessels (see Fig. 2). The streaked appearance of the image in the interior of the blood vessels is an indication of flow. With the intravenous injection of fluorescein, only the blood plasma is fluorescently labeled, red blood cells (and other cellular constituents) are not labeled, and therefore show up as dark patches (32,38). The images shown in Fig. 2 are formed by a progressive line scan of the femtosecond laser beam. If the red blood cells move between successive line scans, they will appear as streaks, with the degree of elongation an indication of red blood cell velocity. Efforts are now underway in this laboratory to use this streak pattern to quantify the blood flow velocity using a method analogous to that used previously with non-progressive line-scan data from capillaries (32).

Clotting of single, near-surface vessels was achieved by focused, single-photon excitation of intravenously injected photosensitizers. Figure 2a shows a branch in a cortical blood vessel, with the region that is to be illuminated with focused 532-nm light indicated by a circle. In Fig. 2b we show the same vessel after 1 min. of 10-mW irradiation with 532-nm light performed before rose bengal was injected into the bloodstream. No change in the blood vessels or qualitative aspects of the flow is apparent, confirming that 532-nm irradiation in the absence of a photosensitizer is not sufficient for clot formation. Figure 2c shows the same vessel after 1 min. of 10-mW irradiation with 532-nm light performed after the intravenous injection of rose bengal. Clot formation in the targeted region is evident (indicated by the arrow). Note that flow continues in the upper branches of the vessel shown in Fig. 2c, and only the in the targeted vessel has flow completely stopped. The secession of flow is characterized by dark patches that remain at a fixed location in time, often surrounded by highly fluorescent patches. The bright regions might be areas where only plasma is present, or might represent cells or other structures that have taken up the dye. The dark patches are likely accumulations of platelets and red blood cells that form the clot.

The dynamics of an arteriole after clot formation is illustrated in Fig. 3. Figure 3a shows the targeted vessel (indicated by a circle) before clotting. The large vessel on the right is a branch of the middle cerebral artery. The blood flow direction in the targeted vessel is away from the middle cerebral artery, from the upper right to the lower left. In Fig. 2b, the vessel has been irradiated for 1 min. at 10 mW with 532-nm light after the intravenous injection of rose bengal. A clot has clearly begun to form in the targeted region (arrow indicates clot). The diameter of the arteriole upstream from the clot has increased to 1.5 times its original diameter. An additional minute of irradiation was performed to further stabilize the clot (Fig. 2c). Two hours after the clot was established this same vessel was imaged again (see Fig. 2d). Blood flow had resumed, and the lumen of the vessel had shrunk in the region of the clot to 75% of its original size. We consistently observed the dilation of vessels upstream from clots. Clot stability over two hours varied, with clots formed consecutively in adjacent branches of the same vessel faring differently.

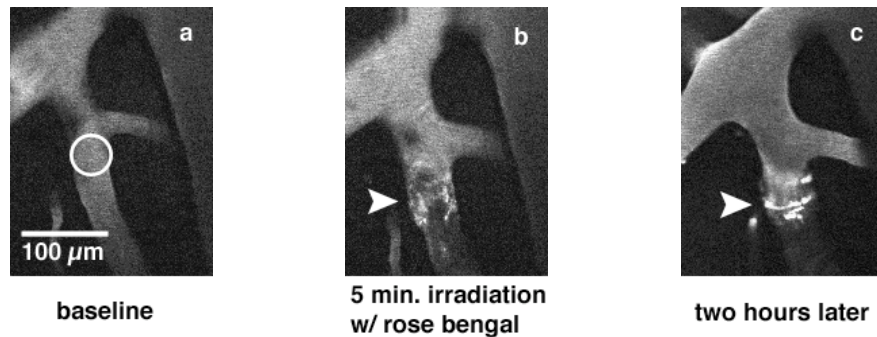


**Fig. 2.** Two-photon laser scanning microscopy image of clot formation in a cortical blood vessel. **a)** Image taken prior to exposure to 532-nm laser light. The streaked appearance of the image in the interior of the blood vessels indicates flow. Red blood cells (not labeled by the intravenously injected fluorescein) appear as dark objects against the fluorescent blood plasma, and their movement between the successive line scans that form the image leads to streaks. The circle indicates the region targeted by the 532-nm laser. **b)** Image taken after exposure to 1 min. of 532-nm laser light at 10-mW average power in the absence of any exogenous photosensitizer. **c)** Image taken after exposure to 1 min. of 532-nm laser light at 10-mW average power after intravenous injection of rose bengal. The clot is formed primarily in the targeted region (clotted region indicated by an arrow).



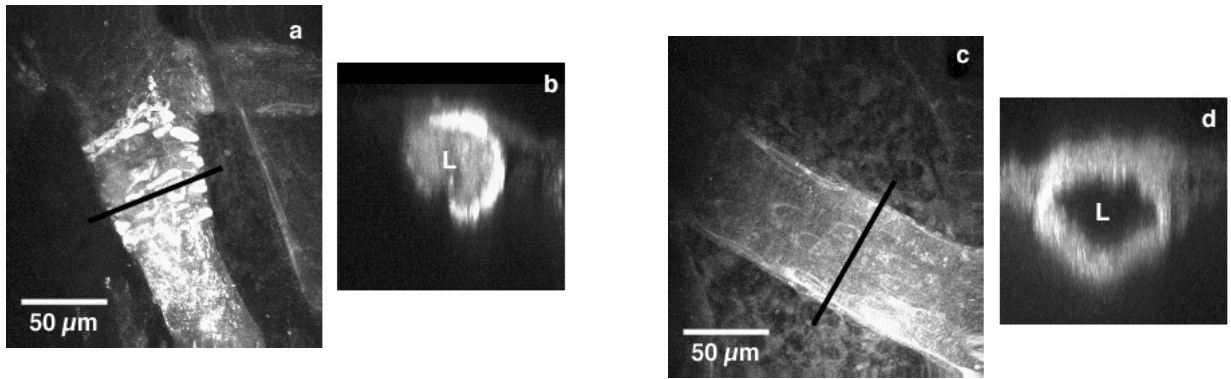
**Fig. 3.** Two-photon laser scanning microscopy images of clotting dynamics in an arteriole. The large vessel on the right of the image is a branch of the middle cerebral artery. Blood flow in the targeted arteriole is from upper right to lower left. **a)** Image taken prior to clot formation. The circle indicates the targeted region. **b)** Image taken after 1 min. irradiation with 10 mW of 532-nm laser light after intravenous injection of rose bengal. Dilatation of the arteriole upstream from the clot is evident. **c)** Image taken after an additional 1 min. of 532-nm irradiation. The clot now appears to completely obstruct the arteriole. The clotted regions in (b) and (c) are indicated by an arrow. **d)** Image of the same arteriole taken two hours after it was clotted. Blood flow is reestablished, and the vessel has contracted in the formerly clotted region.

A clot that remained stable over a two-hour observation time is shown in Fig. 4. Figure 4a shows vessels before irradiation. The large vessel (partially cut-off) on the right is a branch of the middle cerebral artery. The targeted arteriole, which branches off the middle cerebral artery, is indicated by a circle. Flow in this vessel is from top to bottom. Figure 4b shows the vessels after 5 min. of irradiation with 10 mW of 532-nm laser light in 1 min. epochs. The full 5 min. were required for complete occlusion (clot indicated by an arrow). This vessel was clotted nearly one hour after the rose bengal injection, so a low rose bengal concentration in the bloodstream may have contributed to the need for longer-duration illumination to form a clot. After clot formation, the branching arteriole just above the clot and going to the right dilated to 1.5 times its original diameter. Figure 4c shows the clot two hours later, with no further irradiation. In this case, the clot has stabilized (clot indicated by an arrow). The brightly labeled, punctate objects in the vicinity of the clot are likely perivascular microglial cells. These cells are known to be autofluorescent or they could have taken up the fluorescein-dextran dye along with dead cellular material as a reaction to the local injury (39).



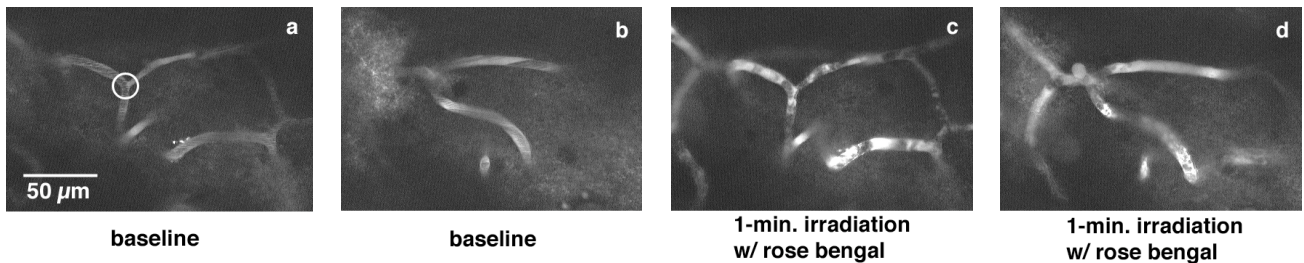
**Fig. 4.** Two-photon laser scanning microscopy images of clotting dynamics in an arteriole. The vessel on the extreme right is a branch of the middle cerebral artery. Blood flow in the targeted arteriole is from top to bottom. **a)** Image taken prior to clot formation. The circle indicates the targeted region. **b)** Image taken after 5 min. irradiation with 10 mW of 532-nm light about one hour after intravenous injection of rose bengal. The clot is indicated by an arrow. **c)** Image taken two hours after clot formation. The clot is still evident (indicated by an arrow).

Figure 5 shows maximal projections of three-dimensional two-photon fluorescence microscopy images of blood vessels in flattened cortex, post mortem after transcardial perfusion of lipophilic fluorescein followed by fixative. The arteriole shown in Fig. 5a is the same one shown in Fig. 4. Figure 5b shows an arteriole from the same rat that was about 2 mm away from any vessels irradiated with 532-nm laser light. The lipophilic dye labels the interior wall of endothelial cells in the blood vessels. In regions where a clot is formed, brightly fluorescent cell processes surround the blood vessel wall (see Fig. 5a). In addition, a cross-sectional view of the clotted vessel shows diffuse fluorescent labeling in the vessel lumen, as shown in Fig. 5b. In contrast, the labeling of an unclotted arteriole lacks the bright punctate staining (see Fig. 5c), and exhibits a clear lumen, with fluorescent labeling confined to the vessel walls (see Fig. 5d). The fluorescent cells surrounding the vessel in Fig. 5a conform to descriptions of perivascular microglial cells identified previously (39). Further histological and immunocytochemical analysis of these clots is underway.



**Fig. 5.** Maximal projections of three-dimensional two-photon fluorescence microscopy images of fixed blood vessels labeled with lipophilic fluorescein. **a)** Image of the same arteriole as in Fig. 4. Strong labeling by the lipophilic fluorescein is evident in the region where the clot was formed. **b)** Cross-sectional view of vessel in (a) showing the obscured lumen (indicated by L) of the vessel in the clotted region. The dark line in (a) indicates the location at which the cross-section was taken. **c)** Image of an arteriole from an unclotted region of the same rat cortex as in (a). Labeling by the lipophilic fluorescein is confined to the vessel walls. **d)** Cross-sectional view of vessel in (c) showing a clear, unobstructed lumen (indicated by L). The dark line in (c) indicates the location at which the cross-section was taken.

The data shown above demonstrate the capability of focused illumination for precise lateral confinement of clot formation. However, the axial confinement of the clot remains in question. Because the rose bengal excitation scheme used here is a single-photon process, we should not expect precise axial confinement. Figure 6 shows laser-induced clotting in a capillary bed. We show a capillary bed with capillaries located approximately 100  $\mu\text{m}$  (Fig. 6a) and 50  $\mu\text{m}$  (Fig. 6b) beneath the surface. The deeper capillaries were targeted (target indicated in Fig. 6a with a circle) with 1 min. irradiation of 1-mW, 532-nm laser light after injection of rose bengal into the bloodstream. The targeted capillaries were clearly clotted (Fig. 6c), as were the capillaries located 50  $\mu\text{m}$  above the target (Fig. 6d). Precise axial confinement of the clot likely requires a nonlinear excitation scheme. We are currently measuring the two-photon absorption cross-sections of several photosensitizer molecules with the aim of implementing a two-photon pumped photothrombotic stroke model.



**Fig. 6.** Two-photon laser scanning microscopy images of laser-induced clotting in capillaries. **a)** Image of the targeted capillary bed located about 100  $\mu\text{m}$  beneath the surface of the brain prior to irradiation. The circle indicates the targeted region. **b)** Image of the capillary bed located 50  $\mu\text{m}$  directly above the capillary bed shown in (a), also prior to illumination. **c)** Image of the capillary bed in (a) after 1 min. irradiation with 1-mW 532-nm laser light after intravenous injection of rose bengal. Flow in all capillaries in the image is stopped. **d)** Image of the capillary bed in (b) after producing the clot in (c). Flow in all capillaries in this plane has also stopped.

## 4. CONCLUSIONS

Photothrombotic clots were formed in individual near-surface cortical blood vessels without obstructing flow in neighboring vessels (see Figs. 2, 3, and 4). We observed vessel dilation upstream from clots (see Figs. 3 and 4), as well as the clearing of clots within hours of induction (see Fig. 3). Although not shown here, we have also observed complete reversals of blood flow direction downstream from clots in both arterioles and venules. In previous work, these localized changes in blood flow and vessel morphology due to blockage of individual vessels have not been examined.

This capability to selectively clot individual vessels and quantitatively observe the response in neighboring vessels is crucial to studies of collateral flow in stroke, i.e., flow reaching a region of the brain by a route not previously utilized. Many of the changes in blood flow conspire to maintain perfusion to regions of the brain downstream from a clot. In experiments aimed at blocking enough vessels to produce an ischemia-induced lesion over one whisker barrel in rat cortex, we found it very difficult to track down all sources of collateral flow and block them. This persistent nature of collateral flow after thrombotic blockage of one, or more, vessels has not been well studied.

Further refinements of our technique will include quantification of blood flow parameters from the laser scanning microscopy images, and possible implementation of two-photon pumping of a photosensitizer to provide axial, as well as lateral, confinement of the clotted volume. Experiments will focus on changes in local blood flow and blood vessels following photothrombotic blockage of individual vessels. Also, the techniques demonstrated here allow for real-time monitoring of the effectiveness of pharmacological therapeutic agents in breaking up and dissolving clots.

## ACKNOWLEDGMENTS

We thank Noah Finkelstein for the loan of laser equipment. This work was funded by the David and Lucille Packard Foundation (D.K.), the National Institute of Health grants NS/041096 (D.K.) and NS/13031 (F.F.E), a La Jolla Interfaces in Science Postdoctoral Fellowship (C.S.), and the National Science Foundation Graduate Fellowship Program (N.N.).

## REFERENCES

1. McBean, D. E. & Kelly, P. A. Rodent models of global cerebral ischemia: a comparison of two-vessel occlusion and four-vessel occlusion. *Gen Pharmacol* **30**, 431-4. (1998).
2. Chen, S. T., Hsu, C. Y., Hogan, E. L., Maricq, H. & Balentine, J. D. A model of focal ischemic stroke in the rat: reproducible extensive cortical infarction. *Stroke* **17**, 738-43. (1986).
3. Tamura, A., Graham, D. I., McCulloch, J. & Teasdale, G. M. Focal cerebral ischaemia in the rat: 1. Description of technique and early neuropathological consequences following middle cerebral artery occlusion. *J Cereb Blood Flow Metab* **1**, 53-60. (1981).
4. Wei, L. et al. Local cerebral blood flow during the first hour following acute ligation of multiple arterioles in rat whisker barrel cortex. *Neurobiol Dis* **5**, 142-50. (1998).
5. Wei, L., Erinjeri, J. P., Rovainen, C. M. & Woolsey, T. A. Collateral growth and angiogenesis around cortical stroke. *Stroke* **32**, 2179-84. (2001).
6. Wei, L., Rovainen, C. M. & Woolsey, T. A. Ministrokes in rat barrel cortex. *Stroke* **26**, 1459-62. (1995).
7. Longa, E. Z., Weinstein, P. R., Carlson, S. & Cummins, R. Reversible middle cerebral artery occlusion without craniectomy in rats. *Stroke* **20**, 84-91. (1989).
8. Lyden, P. D., Jackson-Friedman, C., Shin, C. & Hassid, S. Synergistic combinatorial stroke therapy: A quantal bioassay of a GABA agonist and a glutamate antagonist. *Exp Neurol* **163**, 477-89. (2000).
9. del Zoppo, G. J. Clinical trials in acute stroke: why have they not been successful? *Neurology* **51**, S59-61. (1998).
10. Emsley, H. C. & Tyrrell, P. J. Inflammation and infection in clinical stroke. *J Cereb Blood Flow Metab* **22**, 1399-419. (2002).
11. Overgaard, K. Thrombolytic therapy in experimental embolic stroke. *Cerebrovasc Brain Metab Rev* **6**, 257-86. (1994).
12. Kudo, M., Aoyama, A., Ichimori, S. & Fukunaga, N. An animal model of cerebral infarction. Homologous blood clot emboli in rats. *Stroke* **13**, 505-8. (1982).

13. Krueger, K. & Busch, E. Protocol of a thromboembolic stroke model in the rat: review of the experimental procedure and comparison of models. *Invest Radiol* **37**, 600-8. (2002).
14. Lyden, P. D. et al. Effect of ischemic cerebral volume changes on behavior. *Behav Brain Res* **87**, 59-67. (1997).
15. Lyden, P. D., Zivin, J. A., Chabolla, D. R., Jacobs, M. A. & Gage, F. H. Quantitative effects of cerebral infarction on spatial learning in rats. *Exp Neurol* **116**, 122-32. (1992).
16. Lyden, P. D. & Hedges, B. Protective effect of synaptic inhibition during cerebral ischemia in rats and rabbits. *Stroke* **23**, 1463-9; discussion 1469-70. (1992).
17. Watson, B. D., Dietrich, W. D., Busto, R., Wachtel, M. S. & Ginsberg, M. D. Induction of reproducible brain infarction by photochemically initiated thrombosis. *Ann Neurol* **17**, 497-504. (1985).
18. Dietrich, W. D., Ginsberg, M. D., Busto, R. & Watson, B. D. Photochemically induced cortical infarction in the rat. 2. Acute and subacute alterations in local glucose utilization. *J Cereb Blood Flow Metab* **6**, 195-202. (1986).
19. Dietrich, W. D., Ginsberg, M. D., Busto, R. & Watson, B. D. Photochemically induced cortical infarction in the rat. 1. Time course of hemodynamic consequences. *J Cereb Blood Flow Metab* **6**, 184-94. (1986).
20. Pooler, J. P. & Valenzeno, D. P. Dye-sensitized photodynamic inactivation of cells. *Med Phys* **8**, 614-28. (1981).
21. Herrmann, K. S. Platelet aggregation induced in the hamster cheek pouch by a photochemical process with excited fluorescein isothiocyanate-dextran. *Microvasc Res* **26**, 238-49. (1983).
22. Krammer, B. Vascular effects of photodynamic therapy. *Anticancer Res* **21**, 4271-7. (2001).
23. Pevsner, P. H. et al. A photothrombotic model of small early ischemic infarcts in the rat brain with histologic and MRI correlation. *J Pharmacol Toxicol Methods* **45**, 227-33. (2001).
24. Wester, P., Watson, B. D., Prado, R. & Dietrich, W. D. A Photothrombotic Ring Model of Rat Stroke-in-Evolution Displaying Putative Penumbra Inversion. *Stroke* **26**, 444-450 (1995).
25. Dirnagl, U., Kaplan, B., Jacewicz, M. & Pulsinelli, W. Continuous measurement of cerebral cortical blood flow by laser-Doppler flowmetry in a rat stroke model. *J Cereb Blood Flow Metab* **9**, 589-96. (1989).
26. Busch, E. et al. Reperfusion after thrombolytic therapy of embolic stroke in the rat: magnetic resonance and biochemical imaging. *J Cereb Blood Flow Metab* **18**, 407-18. (1998).
27. Hoehn-Berlage, M. et al. Evolution of regional changes in apparent diffusion coefficient during focal ischemia of rat brain: the relationship of quantitative diffusion NMR imaging to reduction in cerebral blood flow and metabolic disturbances. *J Cereb Blood Flow Metab* **15**, 1002-11. (1995).
28. Ishikawa, M. et al. Platelet adhesion and arteriolar dilation in the photothrombosis: observation with the rat closed cranial and spinal windows. *J Neurol Sci* **194**, 59-69. (2002).
29. Seylaz, J. et al. Dynamic in vivo measurement of erythrocyte velocity and flow in capillaries and of microvessel diameter in the rat brain by confocal laser microscopy. *J Cereb Blood Flow Metab* **19**, 863-70. (1999).
30. Pinard, E., Nallet, H., MacKenzie, E. T., Seylaz, J. & Roussel, S. Penumbra microcirculatory changes associated with peri-infarct depolarizations in the rat. *Stroke* **33**, 606-12. (2002).
31. Denk, W., Strickler, J. H. & Webb, W. W. 2-Photon Laser Scanning Fluorescence Microscopy. *Science* **248**, 73-76 (1990).
32. Kleinfeld, D., Mitra, P. P., Helmchen, F. & Denk, W. Fluctuations and stimulus-induced changes in blood flow observed in individual capillaries in layers 2 through 4 of rat neocortex. *Proceedings of the National Academy of Sciences of the United States of America* **95**, 15741-15746 (1998).
33. Denk, W. et al. Anatomical and Functional Imaging of Neurons Using 2-Photon Laser Scanning Microscopy. *Journal of Neuroscience Methods* **54**, 151-162 (1994).
34. Svoboda, K., Denk, W., Kleinfeld, D. & Tank, D. W. In Vivo Dendritic Calcium Dynamics in Neocortical Pyramidal Neurons. *Nature* **385**, 161-165 (1997).
35. Kleinfeld, D. & Delaney, K. R. Distributed Representation of Vibrissa Movement in the Upper Layers of Somatosensory Cortex Revealed with Voltage-Sensitive Dyes. *Journal of Comparative Neurology* **375**, 89-108 (1996).
36. Grinvald, A., Lieke, E., Frostig, R. D., Gilbert, C. D. & Wiesel, T. N. Functional architecture of cortex revealed by optical imaging of intrinsic signals. *Nature* **324**, 361-4. (1986).
37. Tsai, P. S. et al. in *In Vivo Optical Imaging of Brain Function* (ed. Frostig, R. D.) 113 - 172 (CRC Press, London, 2002).

38. Villringer, A. et al. Confocal laser microscopy to study microcirculation on the rat brain surface in vivo. *Brain Res* **504**, 159-60. (1989).
39. Mato, M. et al. Involvement of specific macrophage-lineage cells surrounding arterioles in barrier and scavenger function in brain cortex. *Proc Natl Acad Sci U S A* **93**, 3269-74 (1996).